Metal Binding Kinetics of Bi-Histidine Sites Used in ψ Analysis: Evidence of High-Energy Protein Folding Intermediates[†]

Gerra L. Bosco,[‡] Michael Baxa,[§,||] and Tobin R. Sosnick*[,‡,§]

The Department of Biochemistry and Molecular Biology, The Institute for Biophysical Dynamics, Computation Institute, and Department of Physics, University of Chicago, Chicago, Illinois 60637

Received November 9, 2008; Revised Manuscript Received February 13, 2009

ABSTRACT: The zinc-specific fluorophore, Zinpyr-1, is used in competition assays to determine the kinetic and thermodynamic parameters of Zn^{2+} binding to engineered bi-histidine sites located in ubiquitin and the B domain of protein A (BdpA). These binding sites are used in ψ analysis studies to investigate structure formation in the folding transition state identified by the change in folding rate upon addition of metal ions. For ubiquitin, the on-rate binding constant and binding affinity for a site located along an α-helix are measured to be $\sim 10^7$ M^{-1} s^{-1} and 3 μM, respectively. For a site located across two β-strands, the metal binding affinity was too weak to measure in the dye competition assays (K_d > 55 μM). The equilibrium-determined values for the Zn^{2+}-induced stabilization of ubiquitin and BdpA match the values derived from changes in the global folding and unfolding rates. Therefore, metal ion binding is in fast equilibrium during the transit over the free energy barrier. Accordingly, the folding rate must be slower than the product of the fractional population of a high-energy intermediate with the metal site formed and the metal binding on-rate constant. The known folding rate of 20 s^{-1} at 1.5 M guanidinium chloride in 400 μM Zn^{2+} provides an upper bound for the stability of such intermediates (ΔG_{U-I} < 4 kcal/mol). These results support a view of the apparent two-state protein folding reaction surface as a fast pre-equilibrium between the denatured state and a series of high-energy species. The net folding rate is a product of the equilibrium constant of the highest-energy species and a transmission rate. For ubiquitin, we estimate the transmission rate to be $\sim 10^4$ s^{-1}. Implications for the role of unfolded chain diffusion on folding rates and barrier heights are discussed.

Metal binding is ubiquitous in biology, being important for folding, stability, transport, and catalysis. Systems utilizing metal ions include metalloregulatory proteins, hemoglobin, tertiary RNAs, transcription factors, and DNA repair machinery. One important example is human prion protein (PrP), which binds metals via histidine residues in an octapeptide repeat (*1*). The conformational change from α-helix to β-sheet associated with amyloid formation in PrP abolishes Zn^{2+} and Mn^{2+} binding while increasing the affinity for nickel and potentially resulting in a loss of metalloregulatory function and the neurotoxicity of prions. The delineation of the kinetic and thermodynamic properties of metal binding proteins is essential in identifying how deficiencies in metal binding can disrupt cellular function and lead to disease.

Many metal binding studies have been conducted using zinc finger proteins, which fold into a DNA binding competent structure upon binding Zn^{2+}. These studies reveal that many metal-binding proteins bind with an on-rate constant between 10^6 (*2, 3*) and 10^9 M^{-1} s^{-1} (*4*−*6*). These rate constants are often measured by competition assays in which prebound cobalt is chased with Zn^{2+} and the dissociation of Co^{2+} is monitored via changes in absorbance at 640 nm (*3*).

In this study, we determine the rate and equilibrium constants of metal binding to the folded and denatured states of two metal binding bi-histidine (biHis)[1] variants of the 76-residue α/β-protein, ubiquitin (Ub). Our study is motivated by the application of ψ analysis (*7*−*13*), a method for characterizing the folding transition state (TS) analogous to mutational ϕ analysis (*14*−*16*). In ψ analysis, biHis metal ion binding sites are individually introduced at known positions throughout the protein to stabilize secondary and tertiary structures. The addition of divalent metal ions stabilizes the interaction between the two known histidine positions. The stabilization is controlled as a continuous function of metal concentration. The degree to which the

[†] This work is supported by a research grant (GM55694) and a training grant (GM007183-32) from the National Institutes of Health.

* To whom correspondence should be addressed. E-mail: trsosnic@uchicago.edu. Phone: (773) 218-5950. Fax: (773) 702-0439.

[‡] The Department of Biochemistry and Molecular Biology.

[§] The Institute for Biophysical Dynamics, Computation Institute.

[||] Department of Physics.

[1] Abbreviations: biHis, bi-histidine; EqComp, equilibrium competition assay; GdmCl, guanidinium chloride; $K_{eq}^{S,N}$, $K_{eq}^{S,U}$, and $K_{eq}^{S,TS}$, metal binding affinity of a biHis site in the native, denatured, and transition state ensemble, respectively; K_{eq}^{U-I}, equilibrium constant of an intermediate; k_{trans}, rate of transmission over the free energy barrier; TSE, transition state ensemble; KinComp, kinetic competition assay; ZP-1, fluorophore Zinpyr-1; k_{on}^{ZP}, on-rate of Zn^{2+} binding to ZP-1; k_{on}^{biHis}, on-rate of Zn^{2+} binding to a Ub biHis site; k_{off}^{biHis}, off-rate of Zn^{2+} binding to a biHis site; Ub, mammalian ubiquitin; BdpA, B domain of protein A; $\Delta\Delta G_{eq}$, change in the free energy of the protein; $\Delta\Delta G_f^{\ddagger}$, change in the free energy of the transition state of a folding pathway.

10.1021/bi802072u CCC: $40.75
Published on Web 02/16/2009

transition state ensemble (TSE) is stabilized by metal ions ($\Delta\Delta G_f^{\ddagger}$) relative to the change in native state stability ($\Delta\Delta G_{eq}$) is quantified with $\psi = (\partial\Delta\Delta G_f^{\ddagger})/(\partial\Delta\Delta G_{eq})$, the instantaneous slope of the Leffler plot of $\Delta\Delta G_f^{\ddagger}$ versus $\Delta\Delta G_{eq}$ (*17*). The slope in the limit of no perturbation (i.e., no metal) is termed the ψ_o value. A ψ_o of 0 or 1 indicates that the biHis site is absent or formed in a nativelike manner in the TSE, respectively.

After measuring ψ values at 14 sites across the protein ubiquitin (Ub), we concluded that Ub's TSE is highly structured with a nativelike topology. In particular, five biHis sites had ψ_o values of unity, indicating nativelike binding affinities in the TSE. These sites define a minimal obligate core consisting of the carboxy terminus of Ub's α-helix and four aligned β-strands. Around this core, another six sites had intermediate ψ_o values, indicative of sites which are fractionally populated or distorted in the TSE (*9, 11, 18*).

Of particular interest here is the mode of metal-induced stabilization of the native state and the TSE. This stabilization reflects the differential ion binding affinity of a biHis site in the denatured state and either the native or the TSE:

$$\Delta\Delta G_{eq}([Me^{2+}]) = -RT\ln\left[\left(1 + \frac{[Me^{2+}]}{K_{eq}^{S,N}}\right)\Big/\left(1 + \frac{[Me^{2+}]}{K_{eq}^{S,U}}\right)\right] \quad (1a)$$

$$\Delta\Delta G_f^{\ddagger}([Me^{2+}]) = -RT\ln\left[\left(1 + \frac{[Me^{2+}]}{K_{eq}^{S,TS}}\right)\Big/\left(1 + \frac{[Me^{2+}]}{K_{eq}^{S,U}}\right)\right] \quad (1b)$$

where $K_{eq}^{S,N}$, $K_{eq}^{S,U}$, and $K_{eq}^{S,TS}$ are the metal ion binding affinities for the biHis site in the native, unfolded, and TS, respectively. For a nativelike site in the TS, $K_{eq}^{S,TS} = K_{eq}^{S,N}$, $\Delta\Delta G_f^{\ddagger} = \Delta\Delta G_{eq}$, and, hence, $\psi_o = 1$.

Rather than measure the metal ion binding affinities directly, we determine the change in equilibrium stability from the change in the folding and unfolding rates of the biHis mutants in the presence of increasing ion concentrations (see Figure 3B in ref *10*)

$$\Delta\Delta G_{eq}([Me^{2+}]) = RT\ln\left[\left(\frac{k_f^{Me^{2+}}}{k_f^0}\right)\Big/\left(\frac{k_u^{Me^{2+}}}{k_u^0}\right)\right] \quad (2)$$

where $k_f^0$and k_u^0 are the folding and unfolding rates in the absence of metal, respectively. Equation 2 implicitly assumes that metal ion binding is in fast equilibrium relative to the overall folding rates. This assumption is supported by the agreement between the equilibrium and kinetically determined values of $\Delta\Delta G_{eq}([Co^{2+}])$ for a biHis site in Ub (a difference of <10%, Figure 2C in ref *10*). That is, ion binding exerts its full thermodynamic effect prior to or during the passage over the kinetic barrier (Figure 1). If equilibration occurs during the passage, then the site must be present often enough that the metal ions are able to bind prior to overall folding

$$k_f < K_{eq}^{U-I} k_{on}^{biHis}[Zn^{2+}] \quad (3)$$

where k_f is the folding rate, K_{eq}^{U-I} is the equilibrium constant for the lowest-energy state where the biHis site is binding competent, and k_{on}^{biHis} is the on-rate of metal binding.

Here we test whether the affinities of the biHis sites determined from the change in stability correspond to the actual binding affinities. We examine biHis binding sites (Figure 1B), site *h* spanning β-sheets β3 and β4 (residues 42 and 70), and site *k* on the N-terminus of the α-helix (residues 24 and 28) with ψ_o values of 0.3 and 0.2, respectively (*10*). The fractional ψ_o values indicate that these sites may be formed near the apex of the free energy reaction surface. We also include results for two helical sites having fractional ψ_o values on the three-helix bundle BdpA (residues 11 and 15, $\psi_o = 0.2$; residues 29 and 33, $\psi_o = 0.5$) (*13*).

The major challenge in our study is that the metal binding of the biHis sites cannot be studied directly. Zn^{2+} is spectroscopically silent as are the standard spectroscopic probes, Co^{2+} and Ni^{2+} with biHis sites (*3, 19*). The bivalent nature of the surface sites impedes their ability to "lock" Co^{2+} or Ni^{2+} into a consensus binding geometry unlike most naturally occurring multivalent sites. The lack of absorbance signal for Zn^{2+} necessitates an indirect approach to measuring metal binding.

Accordingly, we employ a series of kinetic and equilibrium competition measurements to determine metal binding affinities and rates. We use the Zn^{2+}-specific fluorophore, Zinpyr-1 [ZP-1 (Figure 2)], in competition experiments to obtain the metal on-rates and affinities for the biHis sites. We measure the on-rate of Zn^{2+} to the α-helical site in Ub (k_{on}) to be $\sim 3 \times 10^7$ M^{-1} s^{-1} with a binding affinity $K_{eq}^{S,N}$ of ~ 3 μM. Furthermore, the helical site retains some affinity in the unfolded state ($K_{eq}^{S,U} \sim 100$ μM). These binding affinities are quantitatively consistent with the metal-induced stabilization of the protein, determined by changes in either folding rates or equilibrium denaturation profiles. This correspondence indicates that metal binding establishes an equilibrium faster than the overall folding rate. While the affinity of Zn^{2+} for the β-sheet site is too weak to measure in the dye competition assays, the metal-induced stabilization for this site was the same whether measured kinetically (changes in folding rates) or thermodynamically (changes in denaturation midpoint). As discussed above, the associated biHis site must be formed often enough for metal binding to equilibrate. For a biHis site formed in an intermediate near the top of the free energy barrier, this information can be used to assign an upper bound on the stability of the intermediate relative to the unfolded state. Using our measured metal on-rate and eq 3, we estimate the upper bound of the stability of such an intermediate (ΔG_{U-I}) to be <4 kcal/mol.

MATERIALS AND METHODS

Protein Purification. All ubiquitin mutants were purified via expression in BL(21)DE3 cells. Ubiquitin mutants were prepared and purified as previously described (*10*). Verification of the correct ubiquitin mutant is accomplished using mass spectroscopy. All relevant fractions were lyophilized and stored in sealed 50 mL conical tubes at room temperature. The BdpA mutants were prepared in the background of a pseudoWT (F14W/W15Y/N19H) taken from Sato et al. (*35*) (Protein Data Bank entry 1SS1). The purification protocol of the protein mutants was similar to that reported above for ubiquitin. However, the protocol differs in the FPLC step with the Sepharose Fast Flow SP column. The

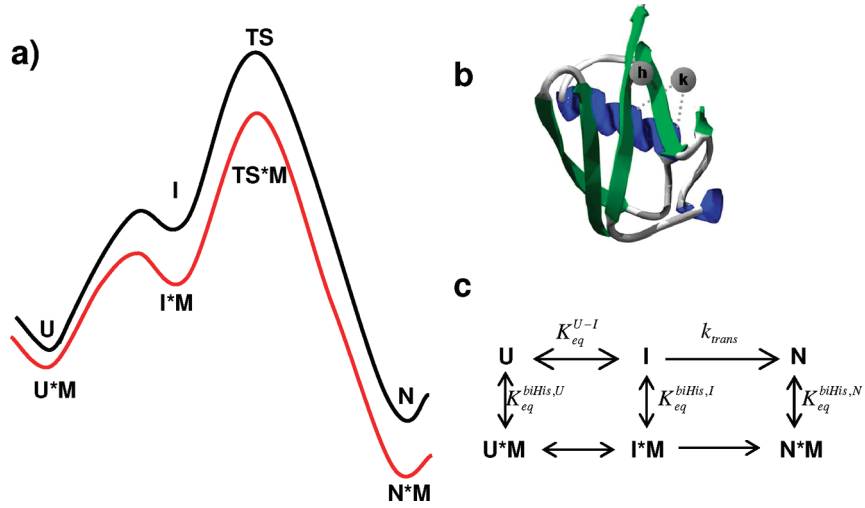

FIGURE 1: biHis sites and protein folding. (a) Folding reaction surface in the absence (black) and presence of M(etal) ions (red). (b) Structure of ubiquitin (Protein Data Bank entry 1UBQ) (*39*) with the locations of site *h* (across β-sheets β3 and β4) and site *k* (at the N-terminus of the α-helix) indicated by the gray circles. Each biHis site is individually introduced into the protein. (c) Proposed thermodynamic cycle for metal binding. The folding rate in the absence of metal ion is given by $k_f = K_{eq}^{U-I} k_{trans}$, while the change in equilibrium stability and folding rate as a function of metal are given by eqs 1b and 2.

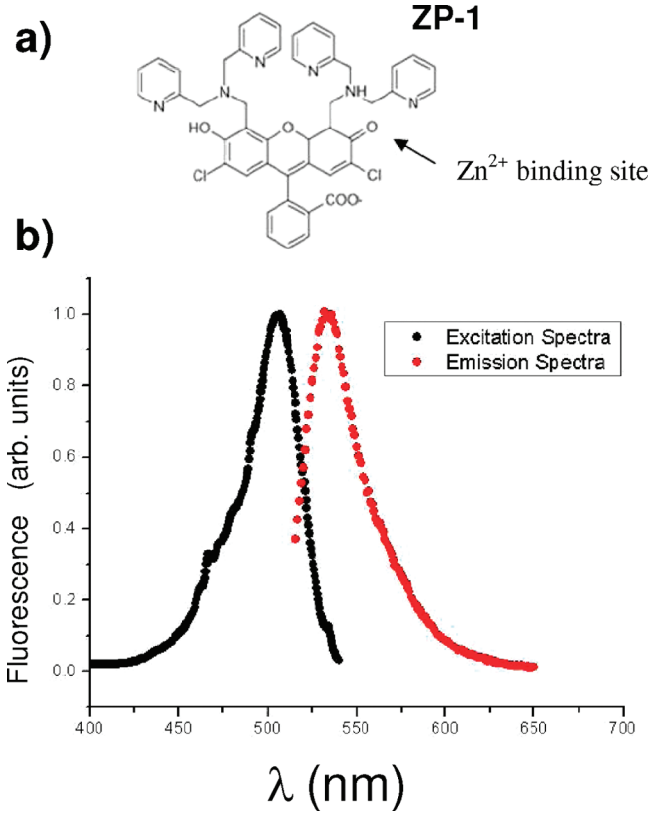

FIGURE 2: Zinc-specific fluorophore, Zinpyr-1. (a) Chemical structure and (b) excitation and emission spectra of ZP-1.

pH of the supernatant from the acid precipitation was not readjusted prior to running over the column, and a dH_2O/0.1% TFA buffer was used to pre-equilibrate the column. The elution of bound protein from the SP column was accomplished using a dH_2O/0.1% TFA/1 M NaCl buffer.

Preparation of Zinc-Specific Fluorophore, Zinpyr-1, Solutions. Zinpyr-1 (ZP-1) is a zinc-specific fluorescent dye with a dissociation constant (K_d) of 1 nM, an excitation maximum of 505 nm, an emission maximum of 530 nm, and a quantum yield (ϕ) of 0.87 when zinc is bound (Neurobiotex) (*36, 37*). ZP-1 was dissolved in DMSO by being vortexed for 10−20 min, and the solution was pulse spun on a tabletop centrifuge to pellet any undissolved particulate. This resulted in a stock concentration of >1 mM, which was then diluted to working concentrations with 50 mM HEPES and 100 mM NaCl (pH 7.5). The concentration of ZP-1 was determined from UV−vis absorbance at 515 nm using an ε of 79500 M^{-1} cm^{-1} (*36, 37*). A 1:2 ZP:Zn^{2+} binding stoichiometry was determined by titration of 1 μM aliquots of Zn^{2+} to an 8 μM ZP-1 solution. The decrease in absorbance at 515 nm was recorded and plotted against the concentration of metal. Similar studies using fluorescence showed a sigmoidal trend, which was not the result of cooperative binding, but an artifact of the increased transmittance of light at higher Zn^{2+} concentrations and the resulting inner-filter effects. The second binding site of ZP-1 has a very weak K_d (~35 μM) and does not significantly bind Zn^{2+} at the low-Zn^{2+} conditions of the current studies (*36*).

Stopped-Flow Measurements. All kinetics data were collected using a rapid mixing BioLogic SFM-4 stopped-flow apparatus equipped with an Oriel mercury arc lamp and Hamamatsu photomultiplier tube with a customized, "delrin" light bevel to decrease reflected incident light. Fluorescence was excited at 283 or 486 nm for ubiquitin folding or ZP-1 metal binding, respectively, and cutoff filters were used to collect fluorescence emission above 310 or 520 nm, respectively. Traces were fit to single- or double-exponential equations using BioLogic Bio-Kine v3.25 software.

Determination of the Rate Constants for Binding of Zn^{2+} to Zinpyr-1. To measure the intrinsic on-rate constant for binding of Zn^{2+} to ZP-1, we performed stopped-flow experiments (as described above) to measure the kinetics of 0.147 μm ZP-1 binding a range of Zn^{2+} concentrations from 0 to 1 mM in the presence of 0, 1.5, or 6 M GdmCl. The concentration of Zn^{2+} stocks was verified by ICP-MS (Stat Analysis Corp., Chicago, IL). The traces were fit to a single-exponential equation and the values of k_{obs} plotted as a function of Zn^{2+} concentration. A linear fit of these data provided the value of the intrinsic bimolecular on-rate constants of ZP-1 binding Zn^{2+} at each concentration of denaturant, which were then used in the global fitting analysis

Table 1: Summary of biHis Binding Constants[a]

	Ub site *h* β-sheet (R42H/V70H)		Ub site *k* α-helix (E24H/A28H)		protein A, α-helix (Q11H/Y15H, N29H/Q33H)[c]	
	$K_{eq}^{S,N}$ (μM)	$K_{eq}^{S,D}$ (μM)	$K_{eq}^{S,N}$ (μM)	$K_{eq}^{S,D}$ (μM)	$K_{eq}^{S,N}$ (μM)	$K_{eq}^{S,D}$ (μM)
change in equilibrium stability	32 ± 3	294 ± 73	3.2 ± 0.2	85 ± 13	16 ± 1	65 ± 6
equilibrium competition	>55[b]	ND	1.8 ± 0.2 (1.5 M)	ND	3.2 ± 0.4 (2.2 M)	ND
kinetic competition	ND[b]	>240	2.5 ± 1.3 (1.5 M)	118.00 ± 0.02 (6 M)	ND	ND

[a] The binding constants for β-sheet site *h* and α-helical site *k* under folding or unfolding conditions are listed for three types of assays: equilibrium stability derived from kinetic folding studies (Figure 3), equilibrium competition (EqComp) (Figure 5), and kinetic competition (KinComp) (Figure 6). Values in parentheses are the GdmCl concentrations at which the measurements were conducted. ND means not determined. The statistical errors are absent for the KinComp measurements as they are not generated by the output of the global fit using DynaFit; the statistical errors for Ub site *k* were obtained from repeated measurements (see Table 2). [b] The binding of Zn^{2+} was indistinguishable from control experiments performed using a Ub variant lacking a biHis site. [c] The change in equilibrium stability was measured with the Q11H/Y15H variant, while the EqComp assays used the N29H/Q33H biHis variant of protein A.

described below. Control experiments with a Ub variant lacking a biHis site indicated that the dye interacts weakly with protein. This interaction increased ZP-1′s fluorescence while decreasing the Zn^{2+} on-rate and binding affinity. It was necessary to wash the lines with buffer after every four to six shots to clear residual ZP-1 from the lines. In rare cases, a mixture of 50% ethanol, 30% methanol, and 10% DMSO, followed by excessive washing with buffer, was needed to fully cleanse the lines.

The on-rate constant and off-rate constant of ZP-1 also were determined by a competition assay with EGTA based on experiments by Jackson et al. (*38*). Using the stopped-flow method to measure kinetics, 20 μM ZP-1 and 20 μM ZnCl were pre-equilibrated and then challenged with 0−10 mM EGTA (data not shown). In the limit of high EGTA, the observed decrease in dye fluorescence is the off-rate of the metal. The kinetic data were fit to single-exponential equations and the resulting k_{obs} values plotted against the concentration of EGTA. The resulting hyperbola was fit according to previously published data (*38*).

Kinetic Competition (KinComp) Experiments. To measure the K_d and rate constants of metal binding to Ub, the three reaction components, ZP-1, Ub, and $ZnCl_2$, were rapidly mixed such that the final concentrations are 3, 0−200, and 1 μM, respectively. In the stopped-flow protocol, the protein and ZP-1 were mixed prior to the addition of $ZnCl_2$. The fluorescence signal was recorded for 0.5−5 s after final mixing. These conditions ensured that the concentration of Zn^{2+} is limiting and, hence, ZP-1 and Ub compete for the metal ion. These experiments were performed in 0, 1.5, and 6 M GdmCl to investigate both folded and denatured state binding. The values of the unknown rate constants, k_{on}^{Ub} and k_{off}^{Ub}, were determined by globally fitting kinetic traces using DynaFit (BioKin Ltd.) (*21*) to the differential equations derived from the reaction depicted in Scheme 1.

For experiments at different GdmCl concentrations, the independently determined values of k_{on}^{ZP} (above) for the appropriate GdmCl concentration (4×10^6 M^{-1} s^{-1} for 0 M GdmCl, 8×10^6 M^{-1} s^{-1} for 1.5 M GdmCl, and 2×10^6 M^{-1} s^{-1} for 6 M GdmCl) were used as the initial values in the fitting process. Although ZP-1 does not bind Zn^{2+} irreversibly, the off-rate is significantly longer than the length of these experiments, and inclusion of k_{off}^{ZP} in the global fit returned a calculated off-rate of 0 while not affecting the other values. As a result, it was subsequently excluded from further calculations. For global analysis of experiments performed at different GdmCl concentrations, the on-rate constant for binding of Zn^{2+} to ZP-1 was set to the value determined by linear titration of Zn^{2+} with ZP-1 in the presence of the appropriate GdmCl concentration. Multiple metal models were tested as well but resulted in fits with large errors and poor residuals, so only the single-zinc model was used. Scripts for the global fit analysis can be requested from the authors.

Equilibrium Competition (EqComp) Experiments. Protein initially at 0−200 μM in 2 μM $ZnCl_2$ was diluted 1:2 upon rapid mixing with 3 μM ZP-1 (final concentration) via the stopped-flow method as described above and the fluorescence recorded for 0.5−5 s. The resulting traces were fit to single-exponential functions, and the resulting k_{obs} was plotted versus Ub concentration. The affinity was determined by fitting k_{obs}([Ub]) with the function given in eq 4.

Equilibrium Measurements. CD measurements were conducted using a Jasco 715 spectropolarimeter with a 1 cm path length. The CD was measured at 222 or 226 nm with a 2−5 nm resolution for 2−10 μM protein. Ub and BdpA measurements were conducted in 50 mM HEPES and 100 mM NaCl at pH 7.5 and 7.7, respectively. Ub and BdpA measurements were carried out at 20 and 10 °C, respectively. Fluorescence excitation and emission spectra of ZP-1 were recorded with a Horiba Jobin Yvon FluoroMax 3 instrument.

RESULTS

Effective Binding Constants from Metal-Dependent Folding Studies. Previous studies on Ub (*10*) found that the change in protein stability as a function of divalent metal ion was described well by the difference between the binding-induced stabilization of the native state and the stabilization of the denatured state, as given by eq 1a. We first tested whether this behavior is maintained in the case of Zn^{2+} for two biHis sites on Ub, site *h* across two β-strands (R42H/V70H) and site *k* on the amino terminus of the α-helix (E24H/A28H). The equilibrium stability as a function of Zn^{2+} concentration is obtained from the changes in the folding and unfolding rates according to eq 2. Values of k_f and k_u are obtained from kinetic measurements under strongly folding or unfolding conditions, either 2−4 or 6 M guanidinium chloride (GdmCl), respectively (data not shown).

The resulting values of $\Delta\Delta G_{eq}([Zn^{2+}])$ are fit to two different models to determine whether ion binding to the denatured state is a significant factor for the two sites (Table 1 and Figure 3). The incorporation of denatured state binding marginally improves the fit to the β-sheet site *h* data. The native binding affinity ($K_{eq}^{S,N}$) is 32 ± 3 μM, while the denatured state binds weakly, if at all ($K_{eq}^{S,U}$ = 294 ± 73

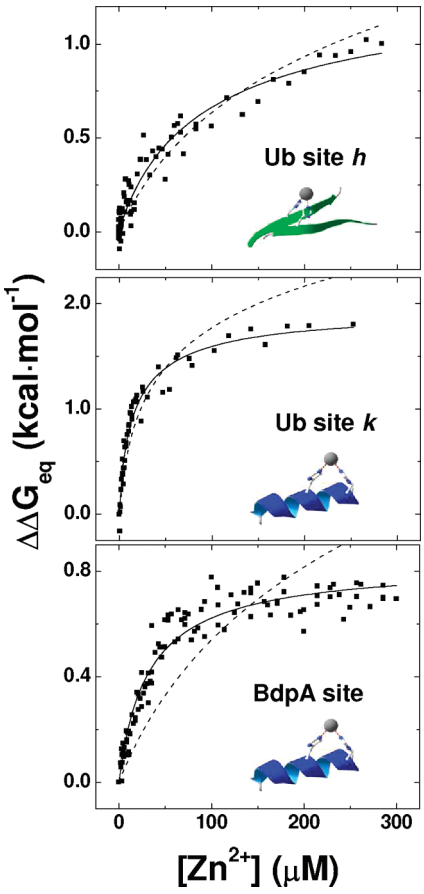

FIGURE 3: Models for metal-dependent changes in protein stability. The protein stability as a function of Zn^{2+} concentration is obtained from the changes in k_f and k_u, for site *h* and site *k* on Ub and a helical site on protein A (Y15H/Q11H). The change in stability is fit to a model allowing for only native state binding (---) and a linked equilibrium binding model allowing for both native and denatured state binding (—). Values are listed in Table 1.

μM). For the α-helical site *k*, however, the inclusion of denatured state binding significantly improves the fit, yielding a $K_{eq}^{S,N}$ of 3.2 ± 0.2 μM and a $K_{eq}^{S,U}$ of 85 ± 13 μM. To test the generality of the results, the measurements are repeated on BdpA with a biHis site on the amino-terminal helix (Q11H/Y15H). Values of k_f and k_u are obtained from kinetic measurements under strongly folding and unfolding conditions, i.e., 2.4 and 5.5 M GdmCl, respectively (data not shown). As with the helical site on Ub, the fit of $\Delta\Delta G_{eq}([Zn^{2+}])$ improves substantially with a model that includes denatured state binding with the following affinities: $K_{eq}^{S,N} = 16 \pm 1$ μM, and $K_{eq}^{S,U} = 65 \pm 6$ μM.

Metal Binding Is in Fast Equilibrium. To investigate whether the binding of metal ions to biHis sites is in fast equilibrium relative to overall folding rates, we compared the values of the equilibrium stability determined from the aforementioned changes in folding rates to the values obtained by equilibrium chemical denaturation measurements. The GdmCl denaturation profiles are obtained for multiple Zn^{2+} concentrations (Figure 4, inset). For both Ub sites, the equilibrium and kinetically determined values of $\Delta\Delta G_{eq}([Zn^{2+}])$ are in very good agreement with a deviation of less than 0.2 kcal/mol. For the eight biHis sites located on the three helices of BdpA, the stability increased between 0.3 and 1.7 kcal/mol in the presence of 1 mM Zn^{2+} (*13*). Nevertheless, for any given site, the equilibrium and kinetically determined values are very similar (deviation of <0.2 kcal/mol). Hence, prior to or during the passage over the kinetic barrier, metal ion binding is able to exert its full thermodynamic effect on the weakly populated intermediates containing a binding competent biHis site.

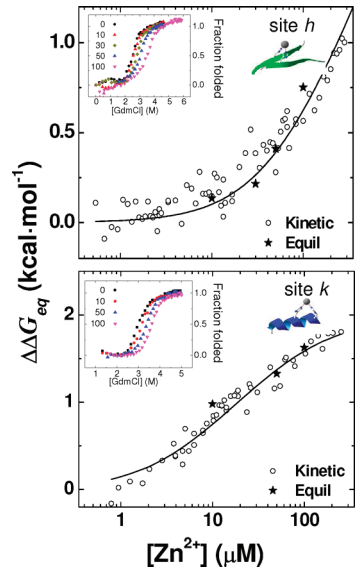

FIGURE 4: Metal binding is in fast equilibrium. For Ub, the equilibrium stabilities determined by equilibrium denaturant profiles (★) agree with the values obtained from the changes in k_f and k_u (○) according to eq 2. The insets show the equilibrium denaturant melts for each site as measured by CD at 226 ± 5 nm normalized to the value of the native and denatured states, as a function of Zn^{2+} concentration (values in micromolar). The measurements were conducted in 50 mM HEPES and 100 mM NaCl (pH 7.5).

Determination of Metal Binding Equilibrium and Rate Constants. To directly measure the metal binding affinity for a biHis site, the zinc-specific fluorophore ZP-1 is used in competition assays. This fluorophore is based on the quinoline family of metal-specific fluorophores (Figure 2a). Metal-binding fluorophores such as Zinpyr-1 were originally developed for measuring the intracellular concentration and localization of metals *in vivo* via fluorescence microscopy. In this study, however, we utilize the high specificity and affinity of ZP-1 for Zn^{2+} to act as a sink for free Zn^{2+} in kinetic and equilibrium competition assays.

Upon chelation of a single zinc ion, ZP-1's excitation and emission maxima are 505 and 520 nm, respectively (Figure 2b). The bimolecular on-rate constant for binding of Zn^{2+} to ZP-1, k_{on}^{ZP}, is obtained by measuring the rate of formation of the ZP-1−Zn^{2+} complex over a range of (excess) Zn^{2+} concentrations. Each of the reaction curves is fit to a single exponential to yield the apparent rate constant, k_{obs} (data not shown). The slope of a linear fit of $k_{obs}([Zn^{2+}])$ yields a bimolecular on-rate constant (k_{on}^{ZP}) of (3.7 ± 0.1) × 10^6 M^{-1} s^{-1} in 0 M GdmCl.

The binding of Zn^{2+} to ZP-1 depends on buffer conditions. Specifically, the on-rates (k_{on}^{ZP}) in the presence of 1.5 and 6 M GdmCl are (6.8 ± 0.2) × 10^6 and (1.1 ± 0.2) × 10^6 M^{-1} s^{-1}, respectively (data not shown). This nonmonotonic behavior is due to the ionic strength of the buffer, rather than a denaturant effect. Measurements are repeated in the presence of NaCl rather than GdmCl. The on-rate constant increases 2-fold until ~2.5 M and then gradually decreases at higher NaCl concentrations (data not shown).

We designed two competition assays using ZP-1 to measure the metal binding affinity for a biHis site on the proteins. The first is an equilibrium competition (EqComp) assay in which 0−300 μM Ub is pre-equilibrated with 1 μM Zn^{2+} before being mixed with 3 μM ZP-1. The second is a kinetic competition (KinComp) assay in which all three components are simultaneously mixed. In the EqComp assays, the fraction of Zn^{2+} not bound to the biHis site prior to the addition of dye, $[Zn^{2+}]_{free}$, determines the initial ZP-1−Zn^{2+} binding rate, k_{obs}. From the decrease in k_{obs}, relative to the rate in the absence of protein, the equilibrium binding constant for the biHis site is determined. In the KinComp assay, however, the observed ZP-1−Zn^{2+} binding rate is influenced by the rate of metal binding to Ub in addition to the binding affinity. The ZP-1−Zn^{2+} on-rate is dependent on the total amount of Zn^{2+}, $[Zn^{2+}]_{total}$, as well as the Ub−Zn^{2+} on- and off-rates.

The concentrations in the EqComp assay are such that $[ZP\text{-}1] = 3[Zn^{2+}]$, a condition where the dye−metal binding rate is under near pseudo-first-order conditions (*20*). The dye−metal off-rate is slow ($k_{off} < 0.01\ s^{-1}$), so formation of the ZP-1−Zn^{2+} complex is effectively irreversible over the course of the measurement. The dye−metal on-rate, k_{obs}, may be approximated by $k_{on}^{ZP}[Zn^{2+}]_{free}$ such that

$$k_{obs} \sim k_{on}^{ZP} \frac{-B + \sqrt{B^2 - 4C}}{2} \quad (4)$$

where $B = K_{eq}^{S} + [Ub]_{total} - [Zn^{2+}]_{total}$, $C = -K_{eq}^{S}[Zn^{2+}]_{total}$, and K_{eq}^{S} is the binding affinity for the biHis site.

The binding of Zn^{2+} to the Ub β-sheet site is considerably weaker (>55 μM) and matches that in control experiments performed with a Ub lacking a biHis site. Therefore, only the results for the α-helical sites are reported under nativelike conditions. For either Ub or BdpA biHis mutants, increasing protein concentrations (up to 300 μM) reduce the observed ZP-1−Zn^{2+} binding rate by nearly 10-fold. The fitting of the observed rates to eq 4 for the helical sites on Ub (in 1.5 M GdmCl) and BdpA (N29H/Q33H, 2.2 M GdmCl) yields binding affinities ($K_{eq}^{S,N}$) of 1.8 ± 0.2 and 3.2 ± 0.4 μM, respectively (Figure 5 and Table 1).

In the KinComp experiments, the protein and Zn^{2+} are not pre-equilibrated but are simultaneously mixed with ZP-1. As a result, the observed ZP-1−Zn^{2+} binding rate depends on both the Zn^{2+} on-rate and its affinity for the biHis site on the protein. The dye binding trace is monitored with increasing concentrations of protein (Figure 6). These experiments are performed in the presence of 1.5 M GdmCl to mimic the conditions of previous metal-dependent folding studies (*10*). The observed rate of formation of the ZP-1−Zn^{2+} complex decreases with an increasing concentration of Ub as the protein reduces the free Zn^{2+} concentration.

To extract kinetic and thermodynamic information from the KinComp experiments, the kinetic modeling software DynaFit (*21*) is used to globally fit these data to the following model: The value of k_{on}^{ZP} is fixed to the value determined from the independent measurements without protein, while the Ub on- and off-rate constants are allowed to vary during the fit. The kinetic parameters for α-helical site *k* are as follows: $k_{on}^{biHis} = (2.7 \pm 2.2) \times 10^7\ M^{-1}\ s^{-1}$, and $k_{off}^{biHis} = 76 \pm 11\ s^{-1}$ (Table 2). The resulting affinity ($K_{eq}^{S,N} = 2.8 \pm 2.3$ μM) is consistent with the value determined in the other measurements (Table 1).

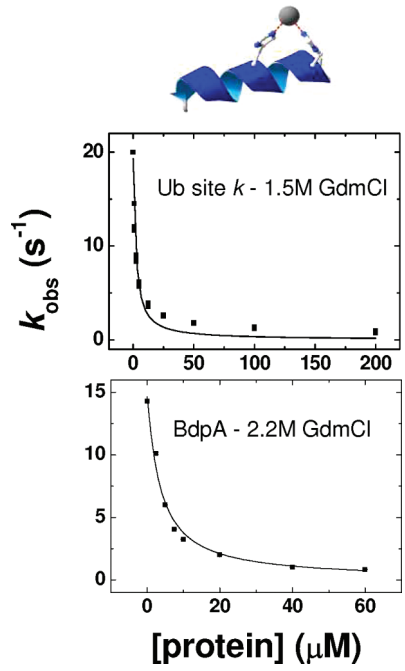

FIGURE 5: biHis binding parameters obtained from equilibrium competition measurements. Observed Zn^{2+}−ZP-1 binding rates, obtained from the change in the dye's fluorescence signal, are obtained when 3 μM ZP-1 (final concentration) is mixed with increasing concentrations of biHis variants of Ub or BdpA that have been pre-equilibrated with 1 μM Zn^{2+} (final concentration). The biHis sites on the proteins reduce $[Zn^{2+}]_{free}$, which reduces the observed rate of formation of the ZP−Zn^{2+} complex according to fluorescence emission of ZP-1 above 520 nm. The binding constants are determined from eq 4.

Investigation of Denatured State Binding. As denatured state metal binding could influence the interpretation of ψ analysis, we directly tested for such binding. As previously discussed, the allowance for both folded and denatured state binding better describes the observed $\Delta\Delta G_{eq}([Zn^{2+}])$ data for the helical site (eq 1a and Figure 3). This improvement suggests that biHis sites can bind metal in the denatured state for α-helical sites. To verify this observation, the rate and equilibrium constants of metal binding to Ub sites *h* and *k* are measured in 6 M GdmCl using KinComp assays (Figure 6 and Table 2) and Scheme 1. Under denaturing conditions, the concentration of β-sheet site *h* does not significantly affect the rate of formation of the ZP-1−Zn^{2+} complex ($K_{eq}^{S,U}$ > 240 μM). The rate of formation of the ZP-1−Zn^{2+} complex decreases in the presence of the α-helical site *k* concentration in both the folded and denatured states; specifically, $K_{eq}^{S,N} = 15.0 \pm 0.3$ μM, and $K_{eq}^{S,U} = 118.00 \pm 0.02$ μM. This retardation in rate indicates that the α-helical site is binding competent in the denatured state and competes with ZP-1.

These values for the binding affinities obtained from the KinComp assays are compared to the values obtained from metal-dependent folding studies and EqComp assays (Table 1). There is significant agreement between all three measurements. As observed in the ZP-1−Zn^{2+} binding experiments, the value of the on-rate constant of Zn^{2+} binding to Ub is slower at 0 M GdmCl than at 1.5 M GdmCl (5×10^6 and $1.7 \times 10^7\ M^{-1}\ s^{-1}$, respectively), which is consistent with

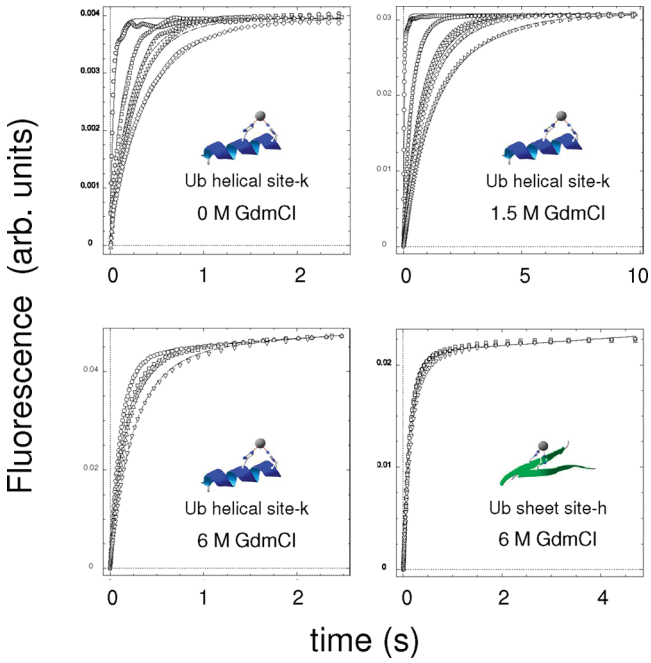

FIGURE 6: Kinetic competition between Zn^{2+} binding to either ZP-1 or biHis sites on the protein in either the folded or unfolded state. The rate of ZP-1 dye binding decreases when 3 μM ZP-1, 1 μM Zn^{2+} (final concentrations), and increasing concentrations of Ub are simultaneously mixed. α-Helical mutant site *k* is either folded (0 or 1.5 M GdmCl) or unfolded (6 M GdmCl), and each trace represents a different Ub concentration. The effect of β-sheet mutant site *h* in 6 M GdmCl is shown as well. The ranges of Ub concentrations used are 33−200 and 0.2−15 μM for β-sheet site *h* and the α-helical site *k*, respectively. The lines are global fits of the data using DynaFit (*21*).

Scheme 1

$$\begin{array}{l} Zn^{2+} + \text{ZP-1} \xrightarrow{k_{on}^{ZP}} \text{ZP-1:Zn} \\ + \\ \text{Ub} \\ k_{on}^{biHis} \downarrow\uparrow k_{off}^{biHis} \\ \text{Ub:Zn} \end{array}$$

Table 2: Kinetic Competition Assays[a]

	Ub site *k* α-helix (E24H/A28H)		
[GdmCl] (M)	k_{on}^{biHis} (μM^{-1} s^{-1})	k_{off}^{biHis} (s^{-1})	K_{eq}^{biHis} (μM)
0	7	92	15
1.5	27 ± 22 (52, 20, 10)	76 ± 11 (88, 74, 66)	2.8 ± 2.3
6	4	471	118

[a] The values of the on- and off-rate constants derived from global fits of five independent experiments at different protein concentrations (see Figures 6 and 7). The binding constant was calculated according to the relationship $K_{eq}^{biHis} = k_{off}^{biHis}/k_{on}^{biHis}$. The statistical errors generally are absent as they not generated by the output of the global fit using Dynafit; the statistical errors listed are obtained from repeated measurements (values in parentheses).

the evidence that metal binding shows a nonmonotonic dependence on ionic strength with affinity peaking at ~2.5 M.

DISCUSSION

In this study, we have employed kinetic and equilibrium competition assays using the zinc-specific fluorophore, Zinpyr-1, to determine the thermodynamic and kinetic constants of Zn^{2+} binding to biHis sites on the surface of Ub and BdpA. Overall, we have seen that the binding affinities measured for the folded state and the denatured state recapitulate the change in global protein stability with metal, $\Delta\Delta G_{eq}([Zn^{2+}])$. This agreement supports our interpretation that the mechanism of metal-induced stability imparted by biHis sites to a protein reflects the difference in the binding affinities in the native and denatured states according to eq 1a.

Our results provide direct evidence that metal can bind to α-helical biHis sites in the denatured state. From the kinetic competition measurements, the α-helical site on Ub was found to have a metal binding affinity of 118 μM in the presence of 6 M GdmCl. In addition, denatured state binding was implicated by the improved fit using the linked equilibrium expression (eq 1a) to the change in stability upon addition of metal for the helical sites on both Ub and BdpA (Figure 2). Metal binding for the β-sheet site was weak under all conditions.

The difference between binding affinity in the denatured state for the helical and sheet biHis sites reflects their difference in sequence proximity. The helical site is sequence local (i, $i + 4$), while the sheet site is nonlocal (i, $i + 28$). The histidines on the two strands are much less likely to be close enough to form a binding competent geometry in an otherwise denatured chain. There is no evidence that the binding for either of these "denatured" structures is native-like, though it seems likely that the two histidines adopt a helical geometry as observed in isolated helices (*22*). However, the possibility that a short β-turn is transiently formed cannot be completely ruled out. For the helical sites, the binding constant at high denaturant concentrations likely represents the metal-induced stabilization of the site scaled by the equilibrium constant for the formation of the site [e.g., a turn of a helix, σ in Zimm−Bragg helix−coil theory (*23*)].

The observed on-rate constant of Zn^{2+} to a preorganized biHis site (k_{on}^{Ub}) is ~10^7 M^{-1} s^{-1}. This value is very similar to that found by Bombarda et al. (3.9 × 10^7 M^{-1} s^{-1}) for bivalent Cys-His sites on HIV NCp7 (*24*) and by Hunt et al. (1 × 10^7 M^{-1} s^{-1}) for biHis sites on wild-type carbonic anydrase (*25*). Studies of other bidentate sites indicate that these sites also bind with micromolar affinity (*2, 3*). The affinities are weaker than the nanomolar to picomolar range found in other Zn binding studies for multidentate binding sites (*4*−*6*).

Metal Ion Binding Is in Fast Equilibrium. For the two and nine measured biHis sites on Ub and BdpA, respectively, the change in protein stability due to Zn^{2+} binding determined by equilibrium denaturation profiles matches those values determined by the changes in the folding kinetics (eq 2). Therefore, ion binding is able to exert its full thermodynamic effect prior to or during the passage over the kinetic barrier. Binding competent states must populate often enough for the metal ions to establish an equilibrium, as given by the inequality in eq 3.

The option of binding metal ions in the denatured state for the helical sites enables this inequality to be readily satisfied. Regardless of whether denatured state binding occurs in the case of high ψ values, the formation of such sites must be relevant for the TSE as they have native or near-native binding affinity by this point on the reaction surface and reduce $\Delta G_f^{\ddagger}$, the height of the kinetic barrier.

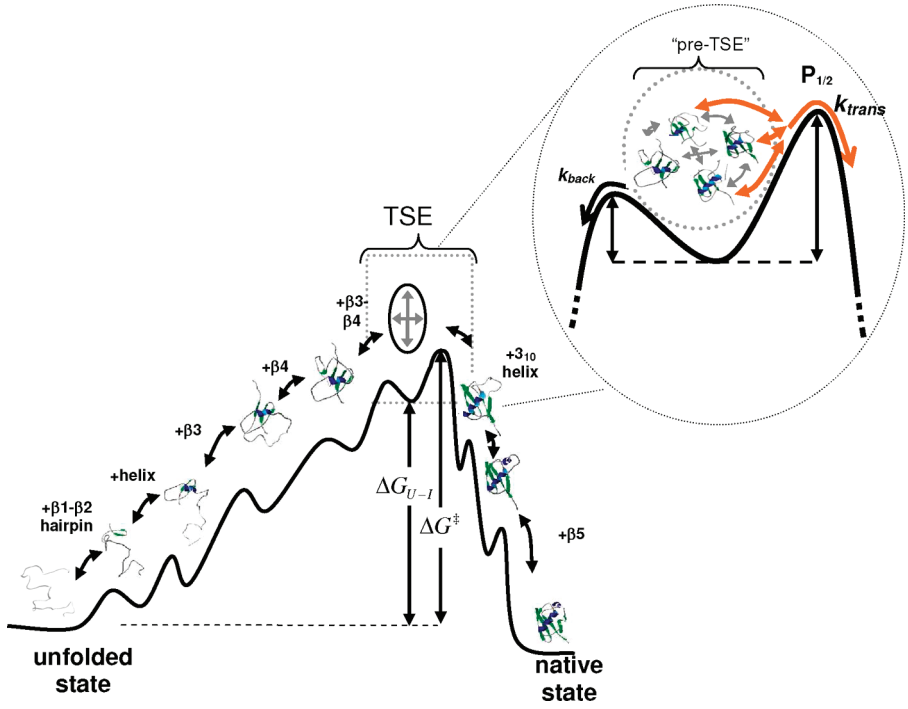

FIGURE 7: Proposed Ub folding pathway placed on a one-dimensional free energy reaction surface. The transition state ensemble (TSE) has a minimal obligate core consisting of the carboxy terminus of the α-helix and four aligned β-strands, as defined by biHis sites having a ψ of 1. Around this core, biHis sites, including sites *h* and *k* studied here, have intermediate ψ values. These values are indicative of sites which are fractionally formed or distorted. The expanded portion highlights the "pre-TSE", which is the thermodynamic well prior to the true $P_{1/2}$ position on the landscape where half the molecules successfully fold to the native state. In the pre-TSE, some of the fractional sites are depicted as additional structure formed in fast equilibrium. From this state, molecules either form more structure and progress forward over the highest point on the reaction surface according to k_{trans} or lose structure and return back toward the unfolded state according to k_{back}. The overall rate of folding is described as $k_f = K_{eq}^{U-I} k_{trans}$, where K_{eq}^{U-I} is the equilibrium constant for the pre-TSE well.

Generally, binding in the denatured state alone is insufficient to generate significant ψ values and does not change their interpretation. A site which produces a kinetic response stabilizes on-pathway folding intermediates and the TSE.

For the long-range β-sheet biHis site, denatured state binding is very weak. Hence, it is unlikely that the denatured state binding can account for the establishment of the ion binding equilibrium prior to folding. For long-range sheet sites with non-zero ψ values, the sites form on the way up the kinetic barrier yet are populated often enough that metal ions can bind and establish a thermodynamic equilibrium.

Folding Landscapes and Barrier Heights. Despite the fact that protein folding is a physically complex process, many experiments over the last few decades have revealed that it is not kinetically complex. For many small proteins, the kinetics are described well by a single exponential, indicative of the free energy surface being dominated by a single barrier (*26*). Crossing this barrier likely requires a series of coordinated events in a largely sequential manner (Figure 7). However, directly examining the transiently populated species on the pre-TS side of a major folding barrier is difficult. The use of biHis sites provides us with an opportunity to explore such events. As the chain traverses the folding landscape, the biHis sites with non-zero ψ values are present often enough to establish a measurable binding affinity. For biHis sites where denatured state binding is inconsequential, folding can be described as series of thermodynamic wells where these biHis sites are formed in fast equilibrium with each other and the denatured state. Further, the associated intermediates establish a rapid pre-equilibrium faster than the overall folding reaction.

We estimate the free energy associated with such a high-energy intermediate formed in rapid pre-equilibrium. β-Sheet site *h* investigated here is an example of such an intermediate. It has a fractional ψ value, binds metal weakly if at all in the denatured state, and likely forms only near the top of the barrier. This site connects strands 3 and 4, the last two elements to associate on the uphill side of the barrier. Since we were unable to directly measure the on-rate for site *h*, we use the measured rate for the helical site as an estimate. Presumably, this estimate is an upper bound since the β-sheet site has a weaker affinity for metal. Using a k_{on}^{biHis} of $\sim 3 \times 10^7$ M^{-1} s^{-1} and a k_f of 20 s^{-1} in 1.5 M GdmCl, we estimate that in 400 μM Zn^{2+}, the intermediate containing this biHis site is formed with an equilibrium constant (K_{eq}^{U-I}) of 0.002 or a ΔG_{U-I} of <4 kcal/mol. Hence, the 4 kcal/mol value provides an estimate of the free energy of a well near the top of the reaction surface.

We stress that the energy of the species is not the absolute barrier height, $\Delta G_f^{\ddagger}$, as the overall barrier height is the energy of the intermediate plus the final kinetic barrier height. Equivalently, the folding rate is given by the rate of crossing the final rate-limiting barrier scaled by the fraction of time the intermediate is formed; i.e., $k_f = K_{eq}^{U-I} k_{trans}$. We use the values given above for k_f and K_{eq}^{U-I} to estimate that $k_{trans} \sim 1 \times 10^4$ s^{-1}. Although the actual event associated with this final step is unknown, information about the Ub pathway garnered from ψ analysis (*10*) suggests a folding event involving either the consolidation of the existing four-strand/helix TS structure defined by the sites with non-zero ψ values or the initial formation of the 3_{10}-helix (the next major structural element to form after the TS). Our k_{trans} rate is

slower than the rate of helix formation for naturally occurring sequences measured by Gai et al. (*27*), which is, in turn, 1 order of magnitude slower than that for alanine-rich helices. Our lower transmission rate may be due to the complicated nature of the remaining folding steps (e.g., the 3_{10}-helix folds from an interior, closed loop).

The view of folding as a series of rapid pre-equilibrium folding events is consistent with clustering analysis of transient species by Shaknovich et al. (*28*) and Pande et al. (*29*) but contrasts with the simpler model of a reaction surface containing only the unfolded and native state wells separated by a single barrier. While the view adopted here may seem to be only a refinement of the simple model, the differences have implications for the estimation of absolute barrier heights from folding rates. Various groups have proposed strategies for elucidating the relationship among the free energy surface, the folding rate, and the height of the major barrier

$$k_f = \frac{\omega_{max}}{2\pi\omega_{min}\tau_o} e^{-\Delta G^{\ddagger}/RT} \quad (5)$$

where ω_{min} and ω_{max} are frequencies that characterize the curvature and ruggedness of the free energy surface in the harmonic well of the unfolded state and at the top of the barrier, respectively (*30*). These efforts are based on extensions of classical transition state theory (TST) (*31, 32*). In classical TST, the height of the barrier is estimated using the Ahrrenius equation, $k = A_o e^{-\Delta G^{\ddagger}/RT}$, where the pre-exponential factor (A_o) is the attempt frequency, which, in the case of protein folding, is the peptide reconfiguration rate (*33*). In the case of rapid pre-equilibrium between the unfolded state and partially folded, high-energy intermediates, the reaction surface's curvature and ruggedness (i.e., diffusion constant) near the unfolded state do not factor into the overall folding rate. Rather, ω_{min} will depend on the properties of the energy well populated just prior to passage across the major barrier.

Schuler et al. (*33*) estimated the free energy barrier using single-molecule FRET in conjunction with Kramers theory assuming a single barrier. On the basis of the rate of collapse in unfolded *Thermotoga maritima* cold shock protein, they estimated the free energy barrier height to be 2−7 kcal/mol, with an attempt frequency between $(0.3\ \mu s)^{-1}$ and $(0.2\ ms)^{-1}$. Studies of the temperature dependence of the folding kinetics and ϕ values of the hYAP WW domain by Gruebele et al. calculated the barrier to be approximately 2.6 kcal/mol (*34*). A direct comparison of these barrier heights with the energy of the species containing biHis site *h* is inappropriate as the intermediate represents a thermodynamic well rather than a barrier height. Nevertheless, we combine the energy of this intermediate with our estimates of $k_{trans} \approx (100\ \mu s)^{-1}$ and $A_o \approx (1\ \mu s)^{-1}$ and calculate an upper bound to the barrier height for ubiquitin; i.e., $\Delta G_f^{\ddagger} < 7$ kcal/mol (in 1.5 M GdmCl).

CONCLUSION

We have developed a method of determining the kinetic and thermodynamic constants for binding of metal to bivalent biHis sites on the surface of ubiquitin and the B domain of protein A. The method can be applied in studying metal binding in systems that cannot be studied by conventional spectroscopic methods. Our experiments gained access to information previously unavailable for weak, bivalent binding sites. We use this information to determine the energetics of pre-transition state conformations of the ubiquitin folding pathway. We find that in 1.5 M GdmCl, a high-energy intermediate with the amino- and carboxy-terminal strands formed exists near the top of the Ub folding reaction surface. The stability of this intermediate (ΔG_{U-I}) is estimated to be <4 kcal/mol (relative to the denatured state).

The concordance between the direct binding measurements and the indirect methods based on changes in protein stability demonstrates that metal binding is described well by a linked equilibrium relating the difference in binding affinities in the folded and denatured states. More importantly, this binding is in fast equilibrium relative to the overall folding rates. Hence, for apparent two-state folding, the simplified reaction surface with a single barrier is better depicted as one containing specific intermediates (i.e., thermodynamic wells) which rapidly equilibrate prior to the final folding step. Due to the rapid pre-equilibrium, states near the top of the major barrier rather than the denatured state determine the relevant chain diffusion constant (i.e., ruggedness of the landscape) in applications of Kramers theory.

ACKNOWLEDGMENT

We thank Profs. S. W. Englander, N. Kallenbach, F. Gai, S. Koide, S. Meredith, P. Kuzmic, and members of our group for comments and discussions.

REFERENCES

1. Jackson, G. S., Murray, I., Hosszu, L. L., Gibbs, N., Waltho, J. P., Clarke, A. R., and Collinge, J. (2001) Location and properties of metal-binding sites on the human prion protein. *Proc. Natl. Acad. Sci. U.S.A. 98*, 8531–8535.
2. Gao, H., Yu, Y., and Leary, J. A. (2005) Mechanism and kinetics of metalloenzyme phosphomannose isomerase: Measurement of dissociation constants and effect of zinc binding using ESI-FTICR mass spectrometry. *Anal. Chem. 77*, 5596–5603.
3. Shi, Y., Beger, R. D., and Berg, J. M. (1993) Metal binding properties of single amino acid deletion mutants of zinc finger peptides: Studies using cobalt(II) as a spectroscopic probe. *Biophys. J. 64*, 749–753.
4. Mely, Y., Cornille, F., Fournie-Zaluski, M. C., Darlix, J. L., Roques, B. P., and Gerard, D. (1991) Investigation of zinc-binding affinities of Moloney murine leukemia virus nucleocapsid protein and its related zinc finger and modified peptides. *Biopolymers 31*, 899–906.
5. Mely, Y., De Rocquigny, H., Morellet, N., Roques, B. P., and Gerad, D. (1996) Zinc binding to the HIV-1 nucleocapsid protein: A thermodynamic investigation by fluorescence spectroscopy. *Biochemistry 35*, 5175–5182.
6. Bombarda, E., Cherradi, H., Morellet, N., Roques, B. P., and Mely, Y. (2002) Zn^{2+} binding properties of single-point mutants of the C-terminal zinc finger of the HIV-1 nucleocapsid protein: Evidence of a critical role of cysteine 49 in Zn^{2+} dissociation. *Biochemistry 41*, 4312–4320.
7. Pandit, A. D., Krantz, B. A., Dothager, R. S., and Sosnick, T. R. (2007) Characterizing protein folding transition states using Psi-analysis. *Methods Mol. Biol. 350*, 83–104.
8. Sosnick, T. R., Krantz, B. A., Dothager, R. S., and Baxa, M. (2006) Characterizing the Protein Folding Transition State Using psi Analysis. *Chem. Rev. 106*, 1862–1876.
9. Sosnick, T. R., Dothager, R. S., and Krantz, B. A. (2004) Differences in the folding transition state of ubiquitin indicated by phi and psi analyses. *Proc. Natl. Acad. Sci. U.S.A. 101*, 17377–17382.
10. Krantz, B. A., Dothager, R. S., and Sosnick, T. R. (2004) Discerning the structure and energy of multiple transition states in protein folding using psi-analysis. *J. Mol. Biol. 337*, 463–475.

11. Krantz, B. A., Dothager, R. S., and Sosnick, T. R. (2004) Erratum to Discerning the structure and energy of multiple transition states in protein folding using psi-analysis. *J. Mol. Biol. 347*, 889–1109.
12. Krantz, B. A., and Sosnick, T. R. (2001) Engineered metal binding sites map the heterogeneous folding landscape of a coiled coil. *Nat. Struct. Biol. 8*, 1042–1047.
13. Baxa, M., Freed, K. F., and Sosnick, T. R. (2008) Quantifying the Structural Requirements of the Folding Transition State of Protein A and Other Systems. *J. Mol. Biol. 381*, 1362–1381.
14. Matthews, C. R. (1987) Effects of point mutations on the folding of globular proteins. *Methods Enzymol. 154*, 498–511.
15. Fersht, A. R., Matouschek, A., and Serrano, L. (1992) The folding of an enzyme. I. Theory of protein engineering analysis of stability and pathway of protein folding. *J. Mol. Biol. 224*, 771–782.
16. Goldenberg, D. P. (1992) Mutational Analysis of Protein Folding and Stability. In *Protein Folding* (Creighton, T. E., Ed.) pp 353−403, W. H. Freeman, New York.
17. Leffler, J. E. (1953) Parameters for the description of transition states. *Science 107*, 340–341.
18. Baxa, M., Freed, K. F., and Sosnick, T. R. (2009) Psi-Constrained Simulations of Protein Folding Transition States: Implications for Calculating Phi. *J. Mol. Biol.* **2009***, 386*, 920–928.
19. Frankel, A. D., Berg, J. M., and Pabo, C. O. (1987) Metal-dependent folding of a single zinc finger from transcription factor IIIA. *Proc. Natl. Acad. Sci. U.S.A. 84*, 4841–4845.
20. Gutfreund, H. (1995) Kinetics for the Life Sciences, pp 60−62, Cambridge University Press, University of Bristol.
21. Kuzmic, P. (1996) Program DYNAFIT for the analysis of enzyme kinetic data: Application to HIV proteinase. *Anal. Biochem. 237*, 260–273.
22. Ghadiri, M., and Choi, C. (1990) Secondary structure nucleation in peptides: Transition-metal ion stabilized α-helices. *J. Am. Chem. Soc. 112*, 1630–1632.
23. Zimm, G. H., and Bragg, J. K. (1959) Theory of the phase transition between helix and random coil in polypeptide chains. *J. Chem. Phys. 31*, 526–535.
24. Bombarda, E., Roques, B. P., Mely, Y., and Grell, E. (2005) Mechanism of zinc coordination by point-mutated structures of the distal CCHC binding motif of the HIV-1 NCp7 protein. *Biochemistry 44*, 7315–7325.
25. Hunt, J. A., and Fierke, C. A. (1997) Selection of carbonic anhydrase variants displayed on phage. Aromatic residues in zinc binding site enhance metal affinity and equilibration kinetics. *J. Biol. Chem. 272*, 20364–20372.
26. Krantz, B. A., Mayne, L., Rumbley, J., Englander, S. W., and Sosnick, T. R. (2002) Fast and slow intermediate accumulation and the initial barrier mechanism in protein folding. *J. Mol. Biol. 324*, 359–371.
27. Mukherjee, S., Chowdhury, P., Bunagan, M. R., and Gai, F. (2008) Folding kinetics of a naturally occurring helical peptide: Implication of the folding speed limit of helical proteins. *J. Phys. Chem. B 112*, 9146–9150.
28. Hubner, I. A., Deeds, E. J., and Shakhnovich, E. I. (2006) Understanding ensemble protein folding at atomic detail. *Proc. Natl. Acad. Sci. U.S.A. 103*, 17747–17752.
29. Singhal, N., Snow, C. D., and Pande, V. S. (2004) Using path sampling to build better Markovian state models: Predicting the folding rate and mechanism of a tryptophan zipper β hairpin. *J. Chem. Phys. 121*, 415–425.
30. Gruebele, M. (2002) Protein folding: The free energy surface. *Curr. Opin. Struct. Biol. 12*, 161–168.
31. Bryngelson, J. D., Onuchic, J. N., Socci, N. D., and Wolynes, P. G. (1995) Funnels, pathways, and the energy landscape of protein folding: A synthesis. *Proteins 21*, 167–195.
32. Jacob, M., and Schmid, F. X. (1999) Protein folding as a diffusional process. *Biochemistry 38*, 13773–13779.
33. Schuler, B., Lipman, E. A., and Eaton, W. A. (2002) Probing the free-energy surface for protein folding with single-molecule fluorescence spectroscopy. *Nature 419*, 743–747.
34. Crane, J. C., Koepf, E. K., Kelly, J. W., and Gruebele, M. (2000) Mapping the transition state of the WW domain β-sheet. *J. Mol. Biol. 298*, 283–292.
35. Sato, S., Religa, T. L., Daggett, V., and Fersht, A. R. (2004) Testing protein-folding simulations by experiment: B domain of protein A. *Proc. Natl. Acad. Sci. U.S.A. 101*, 6952–6956.
36. Burdette, S. C., Walkup, G. K., Spingler, B., Tsien, R. Y., and Lippard, S. J. (2001) Fluorescent sensors for Zn^{2+} based on a fluorescein platform: Synthesis, properties and intracellular distribution. *J. Am. Chem. Soc. 123*, 7831–7841.
37. Woodroofe, C. C., Masalha, R., Barnes, K. R., Frederickson, C. J., and Lippard, S. J. (2004) Membrane-permeable and -impermeable sensors of the Zinpyr family and their application to imaging of hippocampal zinc in vivo. *Chem. Biol. 11*, 1659–1666.
38. Jackson, A. P., Timmerman, M. P., Bagshaw, C. R., and Ashley, C. C. (1987) The kinetics of calcium binding to fura-2 and indo-1. *FEBS Lett. 216*, 35–39.
39. Vijay-Kumar, S., Bugg, C. E., Wilkinson, K. D., Vierstra, R. D., Hatfield, P. M., and Cook, W. J. (1987) Comparison of the three-dimensional structures of human, yeast, and oat ubiquitin. *J. Biol. Chem. 262*, 6396–6399.

BI802072U